White Dwarf and Pre-White Dwarf Pulsations

M. H. Montgomery

Department of Astronomy and McDonald Observatory, University of Texas, Austin TX 78712, USA
Delaware Asteroseismic Research Center, Mt. Cuba Observatory, Greenville, DE, USA

Abstract.
In this review I describe the basic properties of white dwarfs and their pulsations. I then discuss some of the areas in which the pulsations can provide meaningful results, such as internal chemical profiles, possible emission of "exotic" particles, planet detection, crystallization, convection, accretion, and cosmochronology.

Keywords: white dwarfs, oscillations, equation of state
PACS: 97.10.Sj, 97.20.Rp

1. ASTROPHYSICAL CONTEXT

There are two main reasons for studying white dwarf stars. First, white dwarfs represent the final state for about 97% of all stars, so they are by far the most common evolutionary endpoint of stars. Second, their physics is "simpler" than that of main sequence and post-main sequence stars. This makes them useful probes both of their environment (e.g., "How old is the Galaxy?") and of physics (e.g., "How does crystallization occur in a hot, dense plasma?").

Below I list some of the most important aspects of white dwarf physics:

- They are supported by electron degeneracy pressure (due to the Pauli Exclusion Principle)
- Their evolution is simple cooling and is controlled by the heat capacity of their ions and their surface temperature
- When hot ($>$ 25,000 K) they emit more energy in neutrinos than in photons
- As they become very cool ($<$ 7000 K), the ions in the core settle into a crystalline lattice, i.e., they "freeze" or crystallize
- Their gravities are high ($g \sim 10^8$ cm/s^2), so heavy elements sink, producing nearly pure H and He layers (see Figure 1)

The fact that a subset of these stars pulsates allows us to constrain their parameters and internal structure, which in turn allows us to probe physics in an exotic astrophysical environment.

In the following sections I present (an admittedly incomplete) review of the field, with an emphasis on recent work. But first I briefly review the history of the discovery of the various classes.

2. A BRIEF HISTORY

The very first white dwarf pulsator was discovered in 1968 by Arlo Landolt as part of a survey of standard stars [1]. Since this discovery, the observed pulsations in white dwarf stars have been shown to be g-modes [2, 3], with periods typically in the range of 100 to 1000 sec. In the mid-1970's John McGraw, Rob Robinson, and Ed Nather helped show that the known pulsating white dwarfs are single stars with partially ionized H at their surface [4, 5, 6]. This fit with the idea that the pulsations were driven in the partial ionization zone of H. These stars are now known as the DAVs.

Building on this idea, in the early 1980's Don Winget both predicted [7] and discovered [8] that white dwarfs with partially ionized He at their surface pulsated. These stars are the DBVs.

Slightly earlier, in 1979, McGraw et al. [9] discovered the pre-white dwarf variable PG1159-035. This was the inaugural member of the class of hot pre-white dwarf pulsators, the DOVs.

Recently, Montgomery et al. [10] discovered a fourth class of pulsating white dwarf: the DQVs. These stars

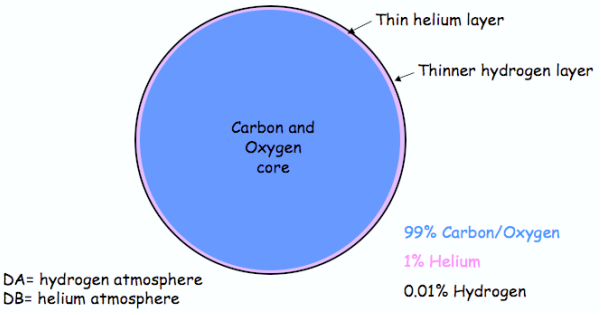

FIGURE 1. A schematic of the structure of a white dwarf star.

have large amounts of C in their atmospheres [11] and, like the DAVs and DBVs, their pulsations seem to be tied to the partial ionization of their dominant surface element, C and/or He.

3. ASYMPTOTIC THEORY OF ADIABATIC PULSATION

The theory of linear, stellar pulsation of spherical stars has been well developed by many authors [e.g., 12, 13, 14]. In addition to assuming that the pulsations are adiabatic (no driving and/or damping), these authors ignore the perturbation of the gravitational potential by the pulsations, the so-called "Cowling approximation" [15]. This has only a small quantitative effect on the pulsations and has the advantage of reducing the pulsation equations to a second-order system in space. A particularly convenient form of the equations mimics that of a vibrating string [13, 14]:

$$\frac{d^2}{dr^2}\psi(r) + K^2\psi(r) = 0, \tag{1}$$

where

$$\psi(r) \equiv \delta P/\rho^{1/2}, \tag{2}$$

$$K^2 \equiv \frac{\omega^2 - \omega_c^2}{c^2} - \frac{L^2}{r^2}\left(1 - \frac{N^2}{\omega^2}\right), \tag{3}$$

and N is the Brunt-Väisälä frequency, $L^2 \equiv \ell(\ell+1)$, c is the sound speed, and ω_c is the acoustic cutoff frequency, which is usually negligible except near the stellar surface.

As we see from equations 1–3, the spectrum of pulsations of a star depends principally on two structural quantities: the Brunt-Väisälä frequency and the Lamb frequency. Since the squares of these quantities relate most directly to the dynamics of the fluid displacements, the symbols N^2 and L_ℓ^2 are often referred to as the Brunt-Väisälä frequency and Lamb frequency, respectively, although they are actually the squares of the respective quantities.

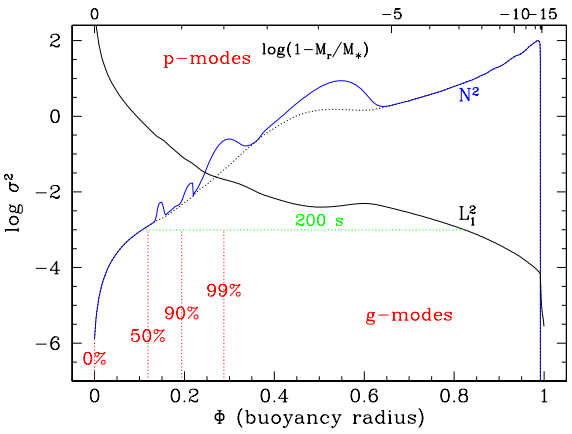

FIGURE 2. Propagation diagram of a DA white dwarf. The Brunt-Väisälä frequency is shown both with (solid curve) and without (dotted curve) the Ledoux term.

A useful tool for investigating the radial extent of a mode is the propagation diagram, an example of which is shown in Figure 2. The N^2 and L_ℓ^2 curves are labeled, and the region of propagation of a 200 second g-mode is shown. In the region between the turning points, denoted by the horizontal dotted line, $K^2(r) > 0$ and the mode has a sinusoidal character; it is said to be "propagating." Beyond these turning points $K^2(r) < 0$, and the mode has an exponential character; in this case it is said to be "evanescent." The top axis displays the traditional radial coordinate $\log(1 - M_r/M_\star)$ whereas the lower x-axis is the normalized "buoyancy radius" $\Phi(r)$, where

$$\Phi(r) \equiv \frac{\int_0^r dr'|N|/r'}{\int_0^{R_\star} dr'|N|/r'}. \tag{4}$$

The coordinate $\Phi(r)$, which was originally introduced by Montgomery et al. [16], is useful for showing how a mode samples the star. In the asymptotic limit, it measures the radius of the star in terms of local wavelengths of the mode.

For the high overtone, low frequency g-modes, $K \sim LN/\omega r$, and the JWKB approximation yields [14]

$$\psi_k(r) = A\frac{1}{\sqrt{K_k(r)}}\sin\left[\phi_k(r) + \frac{\pi}{4}\right], \tag{5}$$

$$\omega_k = \frac{L}{\left(k - \frac{1}{2}\right)\pi}\int_{r1}^{r2} dr\,\frac{N}{r} \tag{6}$$

where

$$\phi_k(r) \equiv \left(k - \frac{1}{2}\right)\pi\,\frac{\int_{r1}^{r} dr'\,|N|/r'}{\int_{r1}^{r2} dr'\,|N|/r'}, \quad k = 1,2,3,\ldots \tag{7}$$

r_1 and r_2 are the inner and outer turning points of the mode, respectively, and k denotes the radial overtone number. We note that when $r_1 \sim 0$ and $r_2 \sim R_\star$, as is commonly the case, we have

$$\phi_k(r) = \left(k - \frac{1}{2}\right)\pi\,\Phi(r). \tag{8}$$

From equation 6 we see that the period spectrum of the modes in the asymptotic limit is

$$P_k = 2\pi/\omega_k$$

$$= \frac{\left(k - \frac{1}{2}\right)2\pi^2}{L}\left[\int_{r1}^{r2} dr\,\frac{N}{r}\right]^{-1} \tag{9}$$

$$\equiv k\Delta P + \varepsilon. \tag{10}$$

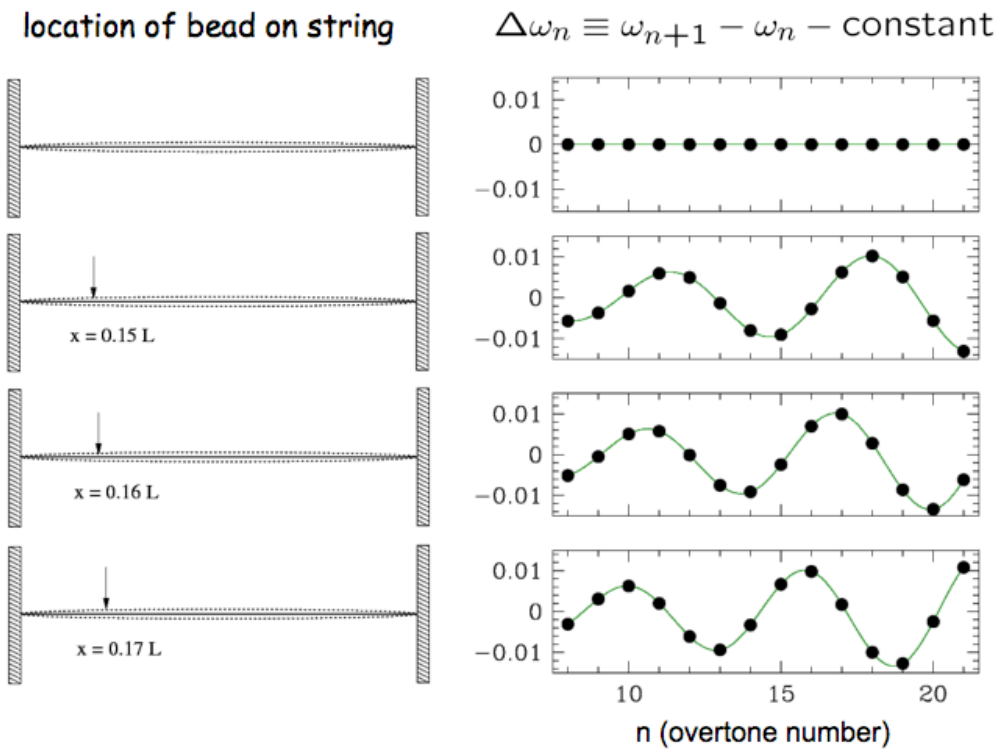

FIGURE 3. Perturbations to the oscillations of a string. The top panels show $\Delta\omega_n$ (right panel) for a uniform string (left panel), and the lower panels show how $\Delta\omega_n$ changes as a bead is placed at the point on the string as indicated in the corresponding left panel.

Thus, in the asymptotic limit the periods are evenly spaced with a separation of

$$\Delta P = \frac{2\pi^2}{L}\left[\int_{r1}^{r2} dr\,\frac{N}{r}\right]^{-1}. \qquad (11)$$

This general form of the period spectrum has been conclusively observed in the DOVs [17] and DBVs [18], and and there is evidence that it is present in the DAVs as well.

4. HOW SEISMOLOGY WORKS

4.1. Analogy with a Vibrating String

Seismology is possible because the eigenfunctions of different modes sample the star differently. To illustrate this most simply we can imagine doing seismology of a vibrating string.

A uniform density vibrating string has a spectrum of eigenfrequencies given by

$$\omega_n = \left(\frac{c\pi}{L}\right) n, \quad n = 1,2,3\ldots \qquad (12)$$

where c is the velocity of transverse waves and L is the length of the string. Thus the frequency spacing of consecutive overtones, $\Delta\omega$, is

$$\Delta\omega \equiv \omega_{n+1} - \omega_n \qquad (13)$$
$$= c\pi/L. \qquad (14)$$

This situation is illustrated in the top panels of Figure 3. If we now imagine placing a (small) bead on the string located $0.15L$ from the left end we find that $\Delta\omega$ is no longer constant. Rather, it has the form shown in the second panel from the top in Figure 3. In the other panels we see that as the bead is moved slightly the shape of $\Delta\omega$ is changed considerably: at $0.17L$ the structure of the frequency spacings is very different than it is at $0.15L$. This demonstrates the potential sensitivity of seismology to probe the internal structure of an object.

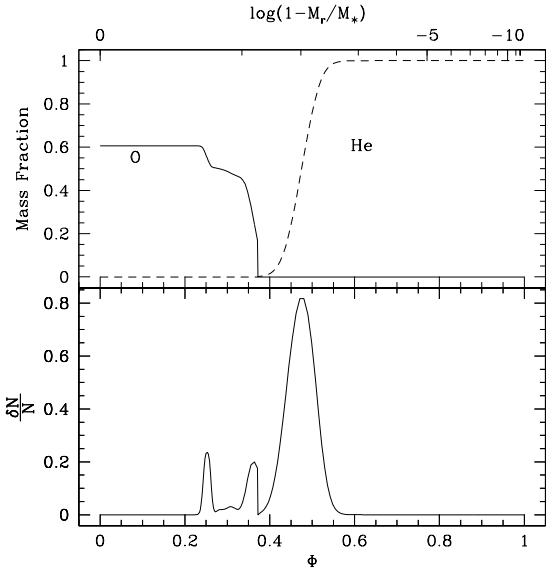

FIGURE 4. "Bumps" in the Brunt-Väisälä frequency (lower panel) as produced by gradients in the chemical profiles for a DB white dwarf model with 0.6 $M_\odot$ and $T_{\rm eff} = 25,000$ K.

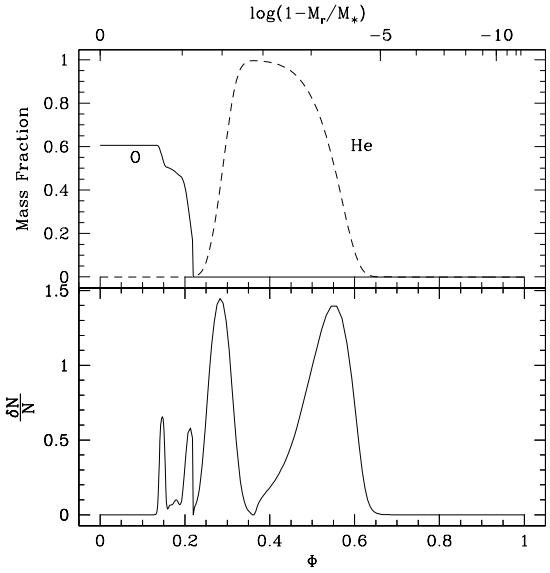

FIGURE 5. "Bumps" in the Brunt-Väisälä frequency (lower panel) as produced by gradients in the chemical profiles for a DA white dwarf model with 0.6 $M_\odot$ and $T_{\rm eff} = 12,000$ K.

The vibrating string is of course not an exact analogy for a pulsating white dwarf, but it does highlight an essential aspect of seismology: the pulsations are sensitive to the "bead," or, rather, they are sensitive to sudden gradients in the structure of the star and our models of it. Since white dwarfs are g-mode pulsators, their periods are sensitive mainly to the Brunt-Väisälä frequency, so "bumps" in N^2 will produce measurable seismological signatures in the observed period spectrum.

The vibrating string analogy also proved its usefulness by leading to the discovery of an approximate symmetry between the core and envelope of models as sampled by g-mode pulsations [16]. This is described more fully in section 4.3.7.

4.2. Application to White Dwarf Models

Figure 4 shows these bumps and their origin for a DB model. The upper panel shows the chemical profiles of oxygen and helium, and the lower panel shows the fractional bumps in the Brunt-Väisälä frequency which the radial gradients in these profiles produce. While the height of these perturbations is important their thinness is actually the most important characteristic for producing oscillatory features in the period spacings (e.g., the "period difference version" of Figure 3). Thus, the narrow bump at $\Phi \sim 0.25$ due to the C/O profile in the core may have as large an effect on the period spacings as the higher and wider bump at $\Phi \sim 0.47$ due to the C/He profile in the envelope.

For contrast, Figure 5 shows the bumps in N^2 for a DA model. Besides the addition of a feature due to the He/H layer, we notice that the other bumps have become narrower and much higher. This is because the chemical gradients in composition transition zones produce an additional term in the Brunt-Väisälä frequency which is largely temperature independent, the "Ledoux term" [e.g., see equation 34 of 19]. The Brunt-Väisälä frequency itself decreases with decreasing temperature, so that $\delta N/N$ for a given bump *increases* in height and *narrows* as the star cools. In the limit that the temperature goes to zero, $N \rightarrow 0$ but δN due to the composition transition zones remains finite, so $\delta N/N \rightarrow \infty$. This is another way of showing that the bumps in N become more pronounced as the star cools.

The bumps in N due to the composition transition zones cause two related things to occur: the periods are no longer equally spaced and the different modes no longer sample the model in the same way. To illustrate what is meant by the latter we show the normalized weight functions for the $17^{\rm th}$ and $18^{\rm th}$ $\ell = 1$ harmonics of a DAV model in Figures 6 and 7, respectively. The $k = 17$ mode has a much larger amplitude in the region $\Phi < 0.2$ than it does in the region $\Phi > 0.2$, whereas the reverse is true for the $k = 18$ mode. It is in this sense that the two modes sample the model differently.

It is common practice to say that such modes are "trapped" on one side or other of the transition zones,

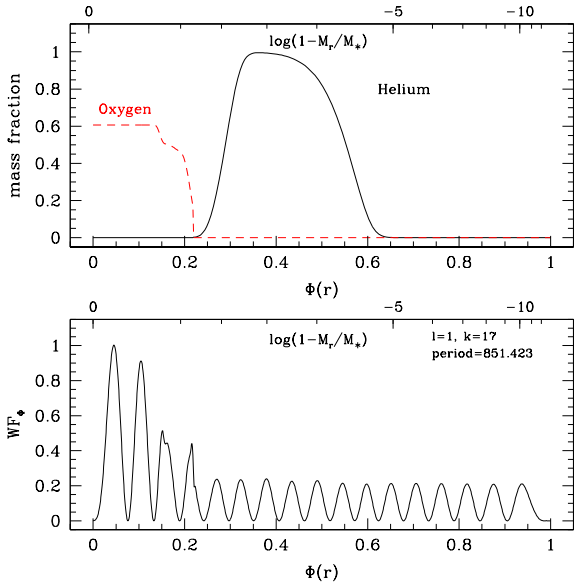

FIGURE 6. The chemical profiles of a DA white dwarf model (top panel) together with the normalized weight function (lower panel) of the 17$^{\rm th}$ $\ell = 1$ overtone mode for a 0.6 $M_{\odot}$ and $T_{\rm eff} = 12,000$ K model.

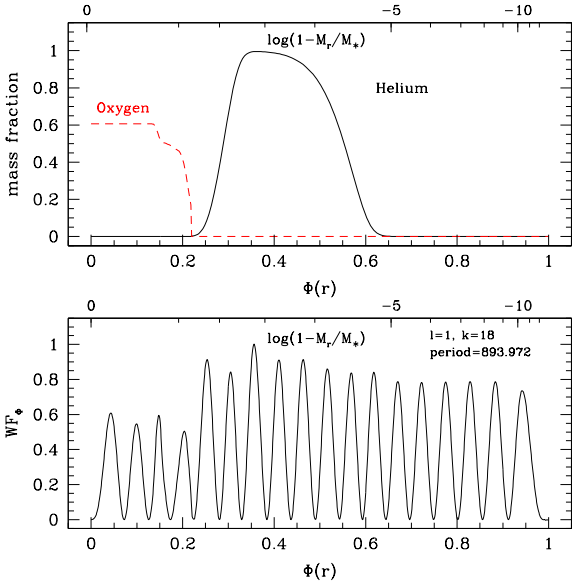

FIGURE 7. The chemical profiles of a DA white dwarf model (top panel) together with the normalized weight function (lower panel) of the 18$^{\rm th}$ $\ell = 1$ overtone mode for a 0.6 $M_{\odot}$ and $T_{\rm eff} = 12,000$ K model.

although this is an unfortunate terminology since the modes can be seen to be propagating, i.e., non-evanescent, on both sides of a given transition zone. What is actually happening is that the suddenness of the transition zones causes waves to be reflected and transmitted, which results in a standing wave pattern with different amplitudes on each side of a given transition zone.

4.3. "Recent" Pulsation Results

In this section I give a review of some of the results to come from white dwarf seismology in the last ten years or so. Given the space and time limitations this list is necessarily incomplete and reflects many of my personal viewpoints and interests.

4.3.1. Driving

Through a combination of new opacities and improved numerics, DOV driving can now be attributed to the partial ionization of carbon and oxygen, acting through the traditional κ mechanism. This was first shown to be a viable explanation for the pulsations in the DOVs by Saio [21] and Gautschy [22]. Since then more refined calculations have been made which strengthen this result [23, 24, 22, 21]. Figure 8 shows the distribution of known

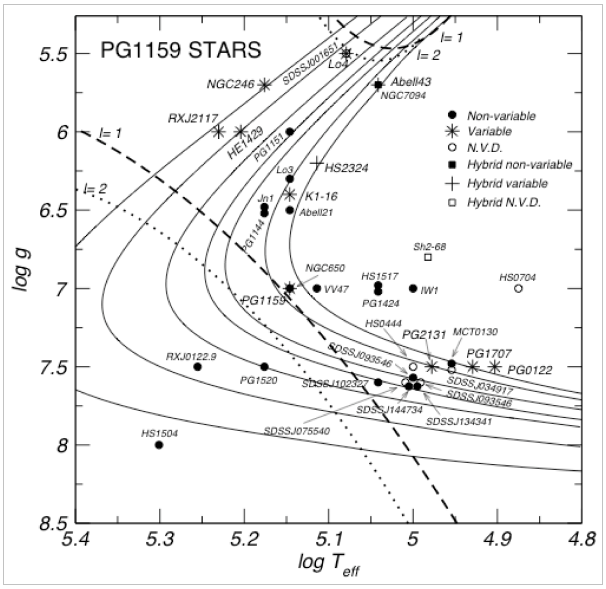

FIGURE 8. The distribution of the spectroscopically calibrated variable and non-variable PG1159 stars in the $\log T_{\rm eff}$–$\log g$ plane. PG1159 stars with no variability data (N.V.D.) are depicted with hollow circles. Solid curves show the evolutionary tracks for different stellar masses: 0.530, 0.542, 0.565, 0.589, 0.609, 0.664 and 0.741 $M_{\odot}$. Parameterizations of the theoretical dipole (dashed curves) and quadrupole (dotted curves) red and blue edges of the instability domain are also displayed. Taken from Córsico et al. [20].

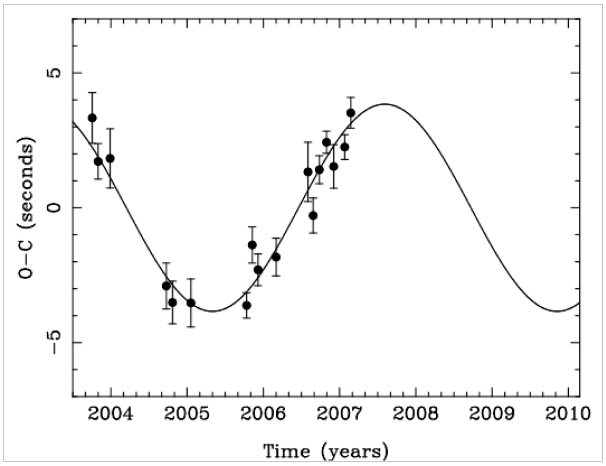

FIGURE 9. O-C diagram for the DAV GD66. The sinusoidal variation in arrival time of the pulses may indicate the presence of an orbiting planet. Taken from Mullally et al. [32].

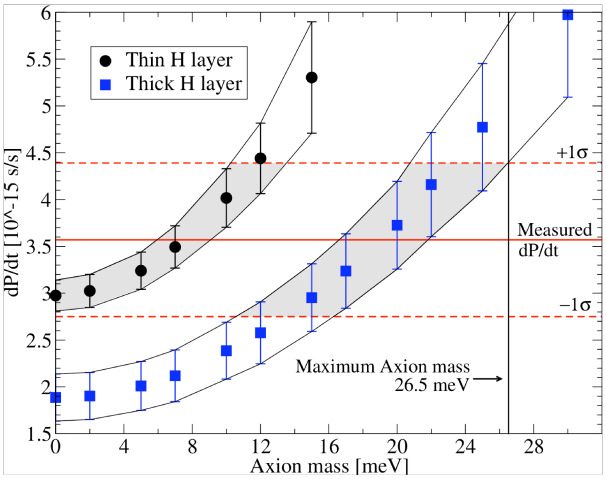

FIGURE 10. Evolutionary calculations of $\dot{P}$ for G117-B15A as a function of the mass of the axion, for both the thick and thin H layer fits. The solid horizontal line shows the observed value and the dashed horizontal lines show the one sigma error bars. Taken from Bischoff-Kim et al. [35].

variable and non-variable PG1159 stars in the $T_{\rm eff}$–$\log g$ plane, with the theoretical boundaries of the instability strip as calculated by Córsico et al. [20].

While the partial ionization of an element (either H or He for the DAVs and DBVs, respectively) is required for the pulsations to be driven, models show that the driving regions of these stars are convective, with the convective flux being much greater than the radiative flux. Thus, the κ mechanism is not relevant for these models. Instead, the most plausible excitation mechanism is "convective driving," or the "Brickhill effect." It was Brickhill [25] who originally showed that the convection zone in these objects would naturally lead to the driving of pulsations with periods greater than $\sim 25\tau_{\rm th}$, where $\tau_{\rm th}$ is the thermal timescale at the base of the convection zone. Later, Wu [26], Wu and Goldreich [27], and Goldreich and Wu [28] gave an analytical description for convective driving, while Ising and Koester [29] expanded on the numerical work of Brickhill and considered synthesized time-dependent spectra in their calculations. It is now generally accepted that this is the dominant excitation mechanism in the DAVs and DBVs [30, 31].

4.3.2. Planet Detection

Several DAVs are known to have pulsations which are stable over long time scales. The champion in this respect is the star G117-B15A, which has a rate of period change $\dot{P} \equiv dP/dt = (3.57 \pm 0.82) \times 10^{-15}$ s/s [33]. Over the 35 year time span it has been observed its period has changed by only about 0.1μs. If such stars harbored planetary systems such as our own, the Jupiter-like planets would induce a wobble in the position of the white dwarf. Due to light-travel-time effects this would produce a periodic variation with an amplitude of a few seconds in the arrival times of individual pulses.

A planet-search survey of such stable pulsators is being conducted at the University of Texas and McDonald Observatory. This survey formed the bulk of F. Mullally's Ph.D. thesis, although it is an ongoing program. One of the early results of this survey is that the DAV GD66 shows indications of a planetary companion [32, 34]. Figure 9 shows the O-C diagram for this star, which exhibits a distinct sinusoidal variation. More data are needed for a full orbit to be seen, so the next year or two will go a long way toward testing the planetary hypothesis.

4.3.3. Exotic Particle "Detection"

This small rate of period change in the DAV G117-B15A is attributed to its natural evolutionary cooling, i.e., $\dot{P}$ is directly related to its energy loss rate. If unseen particles exist which would lead to an accelerated loss of energy, this would increase the measure $\dot{P}$ for this star.

This consequence was pointed out by Winget et al. [36] in the context of the DBVs. Given the relatively high neutrino emission rate in these stars, it should be possible to measure $\dot{P}$ for the stable pulsators and deduce whether the neutrino emission rates are consistent with the Standard Model of particle physics, or whether these rates are in error by factors of order 2. This effect was examined in more detail by Bischoff-Kim [37] and Kim [38], although as yet there are no published measurements of $\dot{P}$

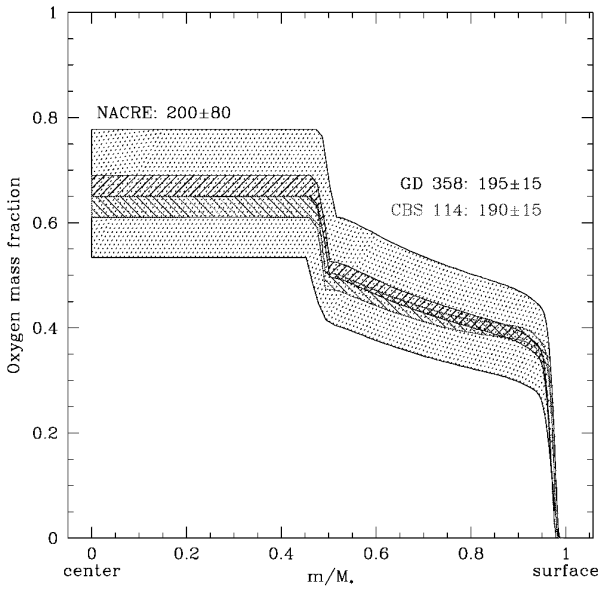

FIGURE 11. The core composition and inferred reaction rates for the $^{12}C(\alpha,\gamma)^{16}O$ reaction rate. Taken from Metcalfe [40].

in a DBV with which to compare.

The DAVs, while emitting insignificant numbers of neutrinos, *could* be sources of axions *if they exist*. Using the measured $\dot{P}$ of G117-B15A, Kim made detailed seismological fits of this star [39] and calculated $\dot{P}$ for a range of masses of the hypothetical axion [35]. As shown in Figure 10, she found two solutions, one of which allowed axions with a mass up to ~ 26 meV. Future seismological investigations may allow us to decide between the two solutions and thus place tighter constraints on the axion mass.

4.3.4. Nuclear Reaction Rates

As shown previously asteroseismology offers us the opportunity to constrain the interior chemical profiles of the pulsating white dwarfs. Since these profiles are the product of nuclear reactions while on the RGB and AGB, they contain information on these reaction rates.

Metcalfe [40] used the set of published periods for two DBVs, GD 358 and CBS 114, in order to perform just such a calculation. As shown in Figure 11, the best-fit C/O profile is consistent with that from evolutionary models with reaction rates in the theoretically predicted range. This is an important confirmation of the ability of seismology to constrain fundamental physical processes.

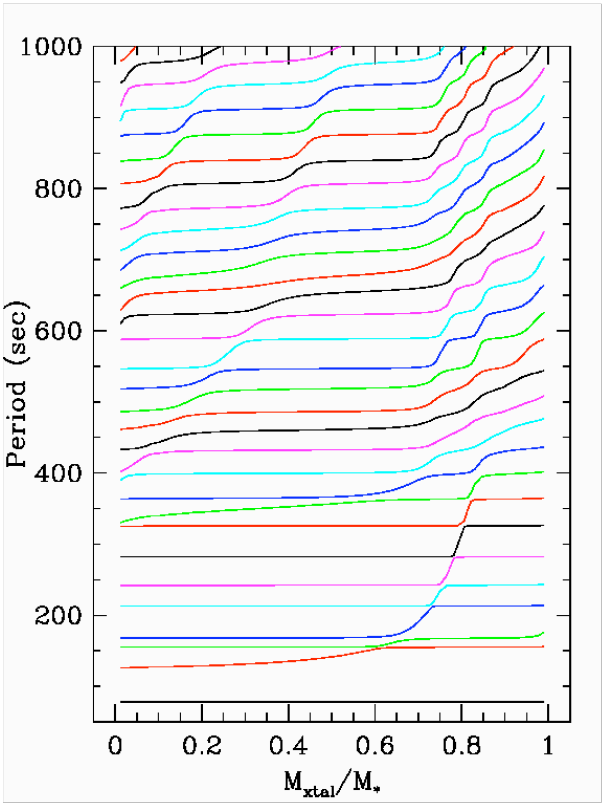

FIGURE 12. Pulsation periods as a continuous function of crystallized mass fraction. Taken from Montgomery [41].

4.3.5. Crystallization

The discovery of pulsations in the DA BPM 37093 [42], together with its high spectroscopic mass of $\sim 1.1\,M_\odot$ [43], opened the possibility of using seismology to probe the physics of crystallization [44]. This is possible because stars of higher mass begin crystallizing at higher temperatures, so the most massive white dwarfs will already be crystallizing at the temperatures found in the DAV instability strip.

Figure 12 shows how the $\ell = 1$ periods (y-axis) of a DAV model change as the crystallized mass fraction (x-axis) is varied. Clearly, crystallization can have a large effect on the spectrum of oscillation periods. Building on this, Metcalfe et al. [45] used seismological fits to constrain the degree of crystallization of this object, citing a value of order $\sim 90\%$ crystallized by mass. In an independent analysis, Brassard and Fontaine [46] found satisfactory fits for a broad range of crystallized mass fraction from 32% to 82%. While both investigations indicate that BPM 37093 should be substantially crystallized, future work will help us resolve this discrepancy and lead to a tighter constraint on crystallization in this object.

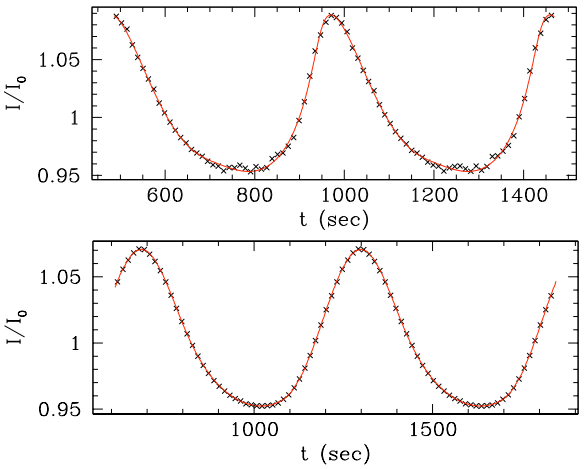

FIGURE 13. *Upper panel:* Nonlinear light curve fit to the nearly mono-periodic DBV PG1351+489. The data was obtained in a WET run in 1995; the light curve has been folded at the period of the main mode, 489 sec. *Lower panel:* Nonlinear light curve fit to the DAV G29-38 in a nearly mono-periodic state in 1988. The data have been folded at the 615 sec dominant periodicity. Taken from Montgomery [47].

4.3.6. Nonlinear Light Curve Fits

Brickhill [48] was the first to demonstrate how the response of the convection zone of a DAV to the pulsations could produce a highly nonlinear light curve, even in the presence of just one pulsation mode. Wu [49] provided an analytical description of this in the weakly nonlinear limit and Ising and Koester [29] enhanced the numerical approach to synthesize time-dependent model spectra.

Montgomery [47] combined the analytical and numerical approaches into a simple numerical model for the nonlinear response of the convection zone to the pulsations. The resulting relatively fast algorithm allowed for direct fits to the light curves of pulsators with highly nonlinear pulse shapes. Such fits are shown in Figure 13. Clearly, the fits (solid lines) are quite accurate at reproducing the data (crosses). The main piece of data retrieved from such fits is the thermal response time of the convection zone, τ_C, which is directly related to the depth of the convection zone. Recently, this technique has been extended to multi-periodic pulsators [50, 51]. By applying this to stars across the DAV and DBV instability strips it should be possible to map out the temperature dependence of the their convection zones independent of the assumed mixing length of convection. In addition to the impact on white dwarfs, these results will provide an important test bed for the next generation of 3D hydrodynamic convection simulations.

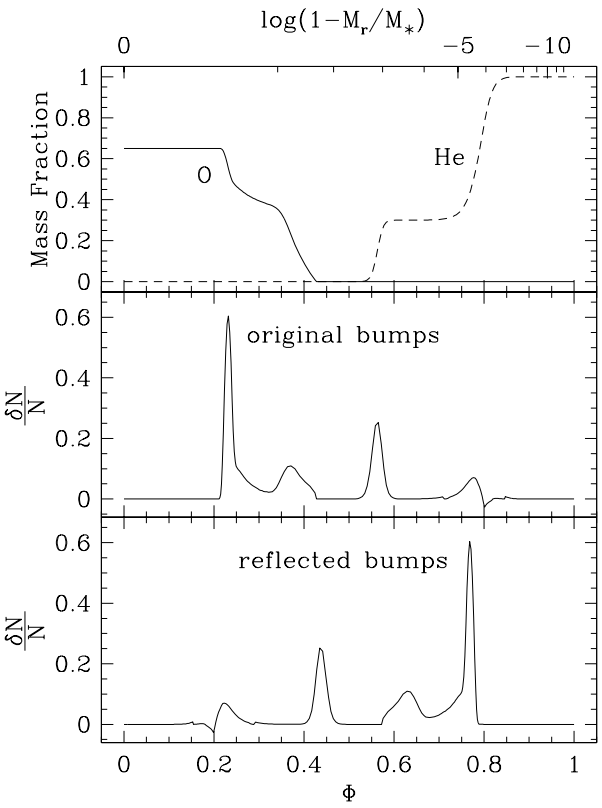

FIGURE 14. The bumps in the Brunt-Väisälä frequency (middle panel) which are produced by given chemical transition zones (upper panel), and the mirror image of these bumps under the reflection mapping (lower panel). Taken from Montgomery et al. [16].

4.3.7. The Core/Envelope Symmetry

In section 4.1 we saw that a vibrating string can be a useful analog for asymptotic g-mode oscillations of a star. Montgomery et al. [16] exploited this close analogy to show that there is an approximate symmetry in the way high overtone oscillations sample the structure in a model, so that features in the core can mimic features in the envelope, and vice versa. Figure 14 shows this effect: to first order the high overtone pulsations would be affected in the same way by the "reflected bumps" as by the original ones. This illustrates how structure in the C/O profile in the core at $\Phi \sim 0.22$ could become entangled with structure in the C/He profile at $\Phi \sim 0.78$. This degeneracy is lifted if modes with different ℓ values are present or if the modes are not yet in the asymptotic limit.

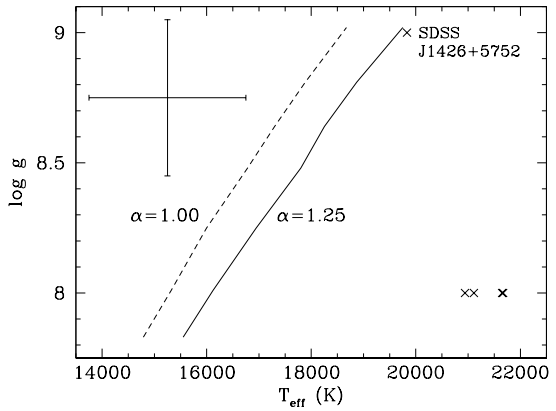

FIGURE 15. A plot of the theoretical blue edge of the carbon-rich instability strip in the $T_{\rm eff}$–$\log g$ plane, assuming ML2/$\alpha = 1.25$ (solid line) and ML2/$\alpha = 1.00$ (dashed line). The crosses give the current best estimates for the positions of the stars observed by Montgomery et al. [10] based on the parameters in Dufour et al. [52]; in the upper left-hand corner we show a representative error bar for these stars.

4.3.8. The DQVs: a New Class of WD Pulsator

One result of the *Sloan Digital Sky Survey* (SDSS) was the discovery of rare objects. One such class is the hot DQ stars, discovered by Dufour et al. [11], which have spectra that are C-dominated. Recently, Montgomery et al. [10] discovered what are apparently g-mode pulsations in one of these objects. Subsequently, two more such DQV stars have been found [53], establishing this as a class of pulsating stars, the first such new class of white dwarf pulsators in 25 years.

Figure 15 shows the blue edge for the DQVs assuming a pure carbon atmosphere; simple time scale arguments were used to derive this so it provides a necessary but not sufficient condition for mode instability to occur. The only star found by [10] to pulsate was SDSS J1426+5752, which encouragingly is the only one of their sample near the predicted blue edge. Since these early results there have been many investigations of the driving mechanism in these stars [e.g., 31, 54].

As a final aside, the prototype of this class has a large magnetic field, of order $\sim$1.2 MG [55]. Thus, it is not only the first pulsating hot DQ star, it is also the first pulsating *magnetic* white dwarf known. This offers us the chance of using the pulsations to better understand the magnetic field, making this star a potential analog of the roAp stars.

4.3.9. Pulsating White Dwarfs in CV Systems

After the discovery of the first known pulsating white dwarf in a cataclysmic variable (CV) system by Warner and van Zyl [56], it was realized that since accretion at a particular rate implied a given amount of heating, for accretion rates in a certain range the surface temperature of the white dwarf could lie in the DAV instability strip [57, 58, 59]. Such systems have been observed in recent years [60, 61] and offer the promise of using the pulsations to provide additional constraints.

4.3.10. Increased Numbers of Known Pulsators

The SDSS was designed to find quasars by looking for faint blue objects. Fortunately for white dwarf researchers, white dwarfs are also blue and faint. As a result, thousands of new white dwarfs have been discovered by the SDSS [62, 63]. After analysis of the DR7 release, Kleinman expects the number of white dwarfs identified to be $\sim 15,000$.

Numerous studies have exploited this data set to identify candidate white dwarf pulsators. For the DAVS, the number known has grown from a pre-SDSS number of about 35 to approximately 150 stars [64, 65, 66, 67, 68]. In addition, the number of known DBVs has increased from a pre-SDSS number of 9 to a current value of 18, doubling the sample of DBVs [69]. While most of these new objects are faint, their pulsations are observable with standard 2m-class telescopes equipped with CCDs. At the very least, these stars will prove useful for delineating the precise boundaries of the instability strips, and they may contain the "rare" pulsators (e.g., DQVs, high-mass pulsators, stable DBVs) which allow us to explore new territory and probe fundamental physics.

5. SUMMARY OF SCIENCE WITH WHITE DWARFS

White dwarf pulsators typically have the richest pulsation spectra aside from that of the Sun. This richness allows asteroseismology to be used, with the result that white dwarf pulsations enable us to:

- Constrain their core chemical profiles
- Look for orbiting extra-solar planets
- Test the properties of "exotic" particles such as plasmon neutrinos and axions
- Constrain the physics of crystallization
- Probe the physics of convection
- Constrain accretion in CV systems

- Improve our white dwarf models for more accurate ages using "white dwarf cosmochronology"

Although the seismology of white dwarfs is well developed, I am certain that there are still many more unexplored avenues which will yield exciting results in the coming years.

ACKNOWLEDGMENTS

I would like to thank Don Winget, Judi Provencal, and the students in the Astronomy stream of the Freshman Research Initiative at the University of Texas for helpful discussions and comments. I am grateful for the financial support of the National Science Foundation under awards AST-0507639 and AST-0909107, and for the support of the Delaware Asteroseismic Research Center.

REFERENCES

1. A. U. Landolt, *ApJ* **153**, 151 (1968).
2. B. Warner, and E. L. Robinson, *Nature* **239**, 2 (1972).
3. E. L. Robinson, S. O. Kepler, and R. E. Nather, *ApJ* **259**, 219 (1982).
4. E. L. Robinson, R. E. Nather, and J. T. McGraw, *ApJ* **210**, 211 (1976).
5. E. L. Robinson, "The observational properties of the ZZ Ceti stars," in *IAU Colloq. 53: White Dwarfs and Variable Degenerate Stars*, edited by H. M. van Horn, and V. Weidemann, 1979, p. 343.
6. J. T. McGraw, *ApJ* **229**, 203 (1979).
7. D. E. Winget, *Gravity Mode Instabilities in DA White Dwarfs.*, Ph.D. thesis, University of Rochester (1982).
8. D. E. Winget, E. L. Robinson, R. D. Nather, and G. Fontaine, *ApJ* **262**, L11 (1982).
9. J. T. McGraw, S. G. Starrfield, J. R. P. Angel, and N. P. Carleton, *SAO Special Report* **385**, 125 (1979).
10. M. H. Montgomery, K. A. Williams, D. E. Winget, P. Dufour, S. DeGennaro, and J. Liebert, *ApJ* **678**, L51 (2008), arXiv:0803.2646.
11. P. Dufour, J. Liebert, G. Fontaine, and N. Behara, *Nature* **450**, 522 (2007), 0711.3227.
12. M. Tassoul, *ApJS* **43**, 469 (1980).
13. F. Deubner, and D. Gough, *ARA&A* **22**, 593 (1984).
14. D. O. Gough, "Linear Adiabatic Stellar Pulsation," in *Astrophysical fluid dynamics*, edited by J.-P. Zahn, and J. Zinn-Justin, Elsevier Science Publishers, Amsterdam, 1993, p. 399.
15. T. G. Cowling, *MNRAS* **101**, 367 (1941).
16. M. H. Montgomery, T. S. Metcalfe, and D. E. Winget, *MNRAS* **344**, 657 (2003), arXiv:astro-ph/0305601.
17. D. E. Winget, R. E. Nather, J. C. Clemens, J. Provencal, S. J. Kleinman, P. A. Bradley, M. A. Wood, C. F. Claver, M. L. Frueh, A. D. Grauer, B. P. Hine, C. J. Hansen, G. Fontaine, N. Achilleos, D. T. Wickramasinghe, T. M. K. Marar, S. Seetha, B. N. Ashoka, D. O'Donoghue, B. Warner, D. W. Kurtz, D. A. Buckley, J. Brickhill, G. Vauclair, N. Dolez, M. Chevreton, M. A. Barstow, J.-E. Solheim, A. Kanaan, S. O. Kepler, G. W. Henry, and S. D. Kawaler, *ApJ* **378**, 326 (1991).
18. D. E. Winget, R. E. Nather, J. C. Clemens, J. L. Provencal, S. J. Kleinman, P. A. Bradley, C. F. Claver, J. S. Dixson, M. H. Montgomery, C. J. Hansen, B. P. Hine, P. Birch, M. Candy, T. M. K. Marar, S. Seetha, B. N. Ashoka, E. M. Leibowitz, D. O'Donoghue, B. Warner, D. A. H. Buckley, P. Tripe, G. Vauclair, N. Dolez, M. Chevreton, T. Serre, R. Garrido, S. O. Kepler, A. Kanaan, T. Augusteijn, M. A. Wood, P. Bergeron, and A. D. Grauer, *ApJ* **430**, 839 (1994).
19. M. Tassoul, G. Fontaine, and D. E. Winget, *ApJS* **72**, 335 (1990).
20. A. H. Córsico, L. G. Althaus, and M. M. Miller Bertolami, *A&A* **458**, 259 (2006), arXiv:astro-ph/0607012.
21. H. Saio, "Linear models for hydrogen-deficient star pulsations," in *Hydrogen Deficient Stars*, edited by C. S. Jeffery, and U. Heber, 1996, vol. 96 of *Astronomical Society of the Pacific Conference Series*, p. 361.
22. A. Gautschy, *A&A* **320**, 811 (1997), arXiv:astro-ph/9606136.
23. A. Gautschy, L. G. Althaus, and H. Saio, *A&A* **438**, 1013 (2005), arXiv:astro-ph/0504495.
24. P.-O. Quirion, G. Fontaine, and P. Brassard, *ApJ* **610**, 436 (2004).
25. A. J. Brickhill, *MNRAS* **251**, 673 (1991).
26. Y. Wu, *Excitation and Saturation of White Dwarf Pulsations*, Ph.D. thesis, California Institute of Technology (1998).
27. Y. Wu, and P. Goldreich, *ApJ* **519**, 783 (1999).
28. P. Goldreich, and Y. Wu, *ApJ* **511**, 904 (1999).
29. J. Ising, and D. Koester, *A&A* **374**, 116 (2001).
30. D. E. Winget, and S. O. Kepler, *ARA&A* **46**, 157 (2008), 0806.2573.
31. G. Fontaine, and P. Brassard, *PASP* **120**, 1043 (2008).
32. F. Mullally, D. E. Winget, S. Degennaro, E. Jeffery, S. E. Thompson, D. Chandler, and S. O. Kepler, *ApJ* **676**, 573 (2008).
33. S. O. Kepler, J. E. S. Costa, B. G. Castanheira, D. E. Winget, F. Mullally, R. E. Nather, M. Kilic, T. von Hippel, A. S. Mukadam, and D. J. Sullivan, *ApJ* **634**, 1311 (2005), arXiv:astro-ph/0507487.
34. F. Mullally, *The Search for Planets around Pulsating White Dwarf Stars*, Ph.D. thesis, The University of Texas at Austin (2007).
35. A. Bischoff-Kim, M. H. Montgomery, and D. E. Winget, *ApJ* **675**, 1512 (2008), arXiv:0711.2041.
36. D. E. Winget, D. J. Sullivan, T. S. Metcalfe, S. D. Kawaler, and M. H. Montgomery, *ApJ* **602**, L109 (2004).
37. A. Bischoff-Kim, *Communications in Asteroseismology* **154**, 16–23 (2008).
38. A. Kim, *Probing Exotic Physics with Pulsating White Dwarfs*, Ph.D. thesis, The University of Texas at Austin (2007).
39. A. Bischoff-Kim, M. H. Montgomery, and D. E. Winget, *ApJ* **675**, 1505 (2008), arXiv:0711.2039.
40. T. S. Metcalfe, *ApJ* **587**, L43 (2003).
41. M. H. Montgomery, *The Evolution and Pulsation of Crystallizing White Dwarf Stars*, Ph.D. thesis, The University of Texas at Austin (1998).
42. A. Kanaan, S. O. Kepler, O. Giovannini, and M. Diaz, *ApJ* **390**, L89 (1992).

43. P. Bergeron, F. Wesemael, R. Lamontagne, G. Fontaine, R. A. Saffer, and N. F. Allard, *ApJ* **449**, 258 (1995).
44. D. E. Winget, S. O. Kepler, A. Kanaan, M. H. Montgomery, and O. Giovannini, *ApJ* **487**, L191 (1997).
45. T. S. Metcalfe, M. H. Montgomery, and A. Kanaan, *ApJ* **605**, L133 (2004).
46. P. Brassard, and G. Fontaine, *ApJ* **622**, 572 (2005).
47. M. H. Montgomery, *ApJ* **633**, 1142 (2005), arXiv:astro-ph/0507444.
48. A. J. Brickhill, *MNRAS* **259**, 519 (1992).
49. Y. Wu, *MNRAS* **323**, 248 (2001), arXiv:astro-ph/0003101.
50. M. H. Montgomery, *Communications in Asteroseismology* **154**, 38 (2008).
51. M. H. Montgomery, "Using Non-Sinusoidal Light Curves of Multi-Periodic Pulsators to Constrain Convection," in *Astronomical Society of the Pacific Conference Series*, edited by A. Napiwotzki, and M. R. Burleigh, 2007, vol. 372 of *Astronomical Society of the Pacific Conference Series*, p. 635.
52. P. Dufour, G. Fontaine, J. Liebert, G. D. Schmidt, and N. Behara, *ApJ* **683**, 978 (2008), 0805.0331.
53. B. N. Barlow, B. H. Dunlap, R. Rosen, and J. C. Clemens, *ApJ* **688**, L95 (2008), 0810.2140.
54. A. H. Córsico, A. D. Romero, L. G. Althaus, and E. García-Berro, *ArXiv e-prints* (2009), 0907.3900.
55. P. Dufour, G. Fontaine, J. Liebert, K. Williams, and D. K. Lai, *ApJ* **683**, L167 (2008), 0807.1112.
56. B. Warner, and L. van Zyl, "Discovery of non-radial pulsations in the white dwarf primary of a cataclysmic variable star," in *New Eyes to See Inside the Sun and Stars*, edited by F.-L. Deubner, J. Christensen-Dalsgaard, and D. Kurtz, 1998, vol. 185 of *IAU Symposium*, p. 321.
57. P. Arras, D. M. Townsley, and L. Bildsten, *ApJ* **643**, L119 (2006), arXiv:astro-ph/0604319.
58. D. M. Townsley, P. Arras, and L. Bildsten, *ApJ* **608**, L105 (2004), arXiv:astro-ph/0405132.
59. D. M. Townsley, and L. Bildsten, *ApJ* **596**, L227 (2003), arXiv:astro-ph/0309208.
60. A. S. Mukadam, B. Gaensicke, D. M. Townsley, P. Szkody, L. Bildsten, and E. M. Sion, "Multi-site Observations Of The Accreting White Dwarf Pulsator SDSSJ161033.64-010223.3," in *Bulletin of the American Astronomical Society*, 2008, vol. 40 of *Bulletin of the American Astronomical Society*, p. 530.
61. A. S. Mukadam, P. Szkody, B. T. Gansicke, B. Warner, P. Woudt, E. Sion, D. Townsley, L. Bildsten, J. E. Solheim, O. Fraser, and D. Haggard, "Pulsating white dwarfs in cataclysmic variables," in *Bulletin of the American Astronomical Society*, 2005, vol. 37 of *Bulletin of the American Astronomical Society*, p. 1273.
62. S. J. Kleinman, D. J. Eisenstein, J. Liebert, and H. C. Harris, "The SDSS DR4 White Dwarf Catalog," in *Astronomical Society of the Pacific Conference Series*, edited by A. Napiwotzki, and M. R. Burleigh, 2007, vol. 372 of *Astronomical Society of the Pacific Conference Series*, p. 121.
63. D. J. Eisenstein, J. Liebert, H. C. Harris, S. J. Kleinman, A. Nitta, N. Silvestri, S. A. Anderson, J. C. Barentine, H. J. Brewington, J. Brinkmann, M. Harvanek, J. Krzesiński, E. H. Neilsen, Jr., D. Long, D. P. Schneider, and S. A. Snedden, *ApJS* **167**, 40 (2006), arXiv:astro-ph/0606700.
64. A. S. Mukadam, F. Mullally, R. E. Nather, D. E. Winget, T. von Hippel, S. J. Kleinman, A. Nitta, J. Krzesiński, S. O. Kepler, A. Kanaan, D. Koester, D. J. Sullivan, D. Homeier, S. E. Thompson, D. Reaves, C. Cotter, D. Slaughter, and J. Brinkmann, *ApJ* **607**, 982 (2004).
65. S. O. Kepler, B. G. Castanheira, M. F. O. Saraiva, A. Nitta, S. J. Kleinman, F. Mullally, D. E. Winget, and D. J. Eisenstein, *A&A* **442**, 629 (2005), arXiv:astro-ph/0507490.
66. A. Gianninas, P. Bergeron, and G. Fontaine, *AJ* **132**, 831 (2006), arXiv:astro-ph/0606135.
67. B. G. Castanheira, S. O. Kepler, F. Mullally, D. E. Winget, D. Koester, B. Voss, S. J. Kleinman, A. Nitta, D. J. Eisenstein, R. Napiwotzki, and D. Reimers, *A&A* **450**, 227 (2006), arXiv:astro-ph/0511804.
68. F. Mullally, S. E. Thompson, B. G. Castanheira, D. E. Winget, S. O. Kepler, D. J. Eisenstein, S. J. Kleinman, and A. Nitta, *ApJ* **625**, 966 (2005).
69. A. Nitta, S. J. Kleinman, J. Krzesinski, S. O. Kepler, T. S. Metcalfe, A. S. Mukadam, F. Mullally, R. E. Nather, D. J. Sullivan, S. E. Thompson, and D. E. Winget, *ApJ* **690**, 560 (2009), 0809.0921.